Observation of Turbulent Waves in a Helium Plasma by Optical Spectroscopy

W. R. Rutgers

Association Euratom-FOM, FOM-Instituut voor Plasmafysica, Rijnhuizen, Jutphaas, The Netherlands

(Z. Naturforsch. **30 a**, 1271–1278 [1975]; received June 2, 1975)

From the combined Stark-Zeeman pattern of helium allowed and forbidden optical lines the frequency spectrum, the field strength and the dominant polarization of microfields were determined in a turbulent plasma. Two frequency domains of oscillations were found in a turbulent heating experiment: low-frequency oscillations with dominant polarization perpendicular to the current direction and high-frequency oscillations ($f \sim f_{pe}$) with random polarization. The r.m.s. field strength of the oscillations is between 2 kV/cm and 10 kV/cm. The energy density of turbulent microfields amounts to 1‰ of the thermal energy density.

I. Introduction

In turbulent heating experiments the study of microfields is of great importance because the fluctuation level determines the anomalous resistance, and therefore also the energy flow from ordered drift motion, via field energy to thermal energy. The effect of suprathermal field fluctuations on the line profiles of optical transitions in neutral helium is discussed in detail by Griem [1]. The observation of two-quantum transitions (one plasmon absorbed from or emitted to the plasma plus one photon) was proposed by Baranger and Mozer [2] as a convenient diagnostic method for the determination of the frequency spectrum and strength of electrostatic fluctuations in a plasma. The integrated intensity $S_{\pm}^{BM}$ of satellites at the field frequency, ω, from a forbidden ($\Delta l = 0,2$) transition is calculated in relation to the intensity of a nearby allowed dipole transition ($\Delta l = 1$) for electric fields random in space by second-order time-dependent perturbation theory. The polarization of satellites for non-isotropic fields was calculated by Cooper and Ringler [3]. They also verified the theory in a model experiment, in which a microwave field was applied to a separately generated steady-state helium discharge. A satisfactory agreement between theory and experiment for frequency and strength of the spectroscopically measured and calculated electric field was found.

The deduction of the orientation of the electric fields from the polarization of the satellites is difficult because the fractional polarization is less than 1/7 [3]. The observation of the Zeeman pattern of the satellites is more accurate as was shown by Cooper and Hess [4]. The theory of Baranger and Mozer was extended by Hicks, Hess and Cooper [5] concerning the combined Zeeman and high-frequency Stark effect. The multi-level theory includes multiple quantum transitions and Stark shifts of the energy levels so that the theory remains valid in cases where the intensities of the satellites are not negligibly small. From multi-level theory (Ref. 5) and from different calculations of the effect of a strong field on the spectral lines in a three-level system by Klein, Giraud, and Ben-Reuven [6], it is known under what conditions multiphoton transitions begin to play a role. Under these conditions a monochromatic field $E = E_0 \cos \omega t$ gives rise to satellites at $(2n+1)\omega$ (integer n), symmetrically spaced about the position of a forbidden line and to satellites at $2n \cdot \omega$ about an allowed line. Moreover, a static field lifts the restrictions on a forbidden transition by mixing the eigenstates of a non-perturbed atom. This results in Stark shifts of levels and in an observable "forbidden" line. In recent years the measurement of line profiles was used for spectroscopic observations of plasma oscillations in e.g. a fast theta pinch (Kunze et al. and Davis [7]), a hot ion plasma experiment (Scott et al. [8]), a plasma gun experiment (Matt and Scott [9]) and in a turbulent heating experiment (Schrijver et al. [10]). In all these applications the measured electric field exceeds the value of 5 kV/cm, so that deviations of the strengths of the satellites from the calculated values $S_{\pm}^{BM}$ by Baranger and Mozer [2] can be expected [5, 6].

In this paper a description is given of the measurement of four helium lines, $\lambda = 4922$ Å, 4471 Å, 4026 Å, and 3614 Å, in a turbulent heating experi-

Reprint requests to W. R. Rutgers, FOM-Instituut voor Plasmafysica, Postbus 7, *Jutphaas*, The Netherlands.

Dieses Werk wurde im Jahr 2013 vom Verlag Zeitschrift für Naturforschung in Zusammenarbeit mit der Max-Planck-Gesellschaft zur Förderung der Wissenschaften e.V. digitalisiert und unter folgender Lizenz veröffentlicht: Creative Commons Namensnennung-Keine Bearbeitung 3.0 Deutschland Lizenz.

This work has been digitalized and published in 2013 by Verlag Zeitschrift für Naturforschung in cooperation with the Max Planck Society for the Advancement of Science under a Creative Commons Attribution-NoDerivs 3.0 Germany License.

Zum 01.01.2015 ist eine Anpassung der Lizenzbedingungen (Entfall der Creative Commons Lizenzbedingung „Keine Bearbeitung") beabsichtigt, um eine Nachnutzung auch im Rahmen zukünftiger wissenschaftlicher Nutzungsformen zu ermöglichen.

On 01.01.2015 it is planned to change the License Conditions (the removal of the Creative Commons License condition "no derivative works"). This is to allow reuse in the area of future scientific usage.

ment, together with the deduction of the field strength, the orientation and the frequency spectrum of microfields from the shape of $\lambda = 4922$ Å. A short description of the experiment is given in Section II, followed by the presentation of measurements and the interpretation of helium line profiles in Section III. The problems which appear in the deduction of turbulent field parameters from the measured profiles are discussed in Section IV.

II. Experiment

A description of the turbulent heating experiment was given by Piekaar [11] and Schrijver [12]. Recent results on electron and ion heating, turbulent resistance, microfields and microwave emission are summarized in Ref. 10. It is sufficient to mention that the initial plasma is a hollow-cathode discharge in a magnetic mirror field of 0.45, 0.95 or 1.3 Tesla (at the observation port). The electron temperature is 15 eV and the electron density $8 \cdot 10^{19}\,\mathrm{m}^{-3}$. The plasma is heated up to keV temperatures by a strong current. The turbulent state is excited by discharging a high-voltage capacitor across the length of the plasma column. This results in the growth of ion-acoustic and electron Langmuir oscillations and, consequently, in an anomalously high resistivity accompanied with a high dissipation of energy. Figure 1 gives the current and voltage in a typical helium experiment. The intensity I_A of the "allowed" helium transition $2\,^1P - 4\,^1D$ and I_F of the "forbidden" transition $2\,^1P - 4\,^1F$ is shown in the same picture as a function of time. In Fig. 2 an example of an electron temperature measurement from pulse height analysis of soft X-rays is shown. Electron temperatures up to 10 keV can be obtained within one microsecond. To determine the strength and frequency spectrum of microfields in the plasma we measured four "forbidden" lines, together with nearby "allowed" dipole transitions of neutral helium.

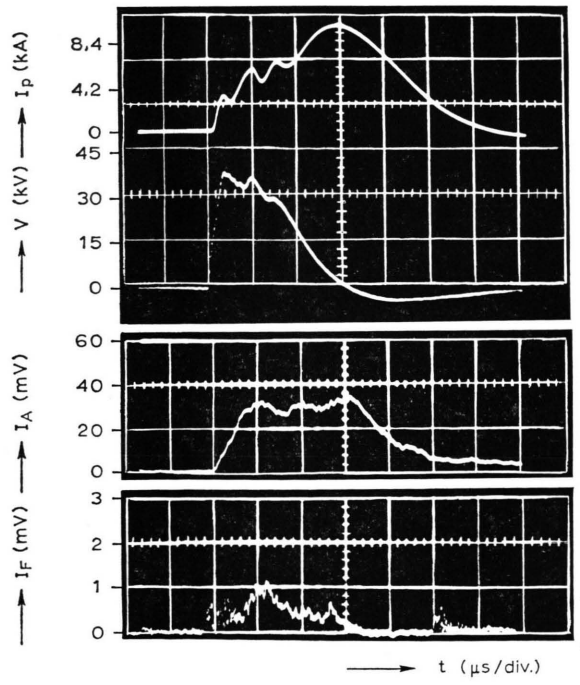

Fig. 1. From top to bottom: discharge current; voltage; intensity of the allowed helium line at 4922 Å; intensity of the forbidden line at 4920 Å.

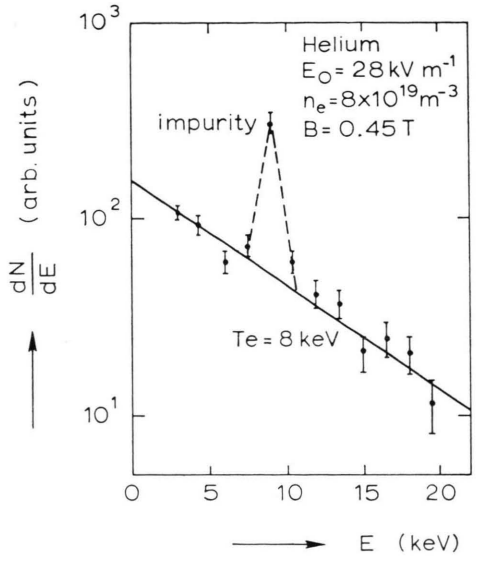

Fig. 2. The electron temperature derived from pulse height analysis of X-ray Bremsstrahlung.

Line profiles were measured with a 1 meter monochromator with a spectral resolution of 0.2 Å. Side-on observations are performed with and without a polarizer in front of the monochromator. The orientation of the polarizer can be parallel to the discharge axis to measure a π spectrum and perpendicular to this axis (σ spectrum).

Table 1.

λ (Å)	transition	Δ (Å)	Δ/ω	$2S_0$ (%)	S_- (%)
4922	$2\,^1P - 4\,^1D$, $4\,^1F$	1.365	2.2	0.288	0.52
4471	$2\,^3P - 4\,^3D$, $4\,^3F$	1.46	2.7	0.172	0.213
4026	$2\,^3P - 5\,^3D$, $5\,^3F$	0.73	1.7	1.62	4.9
3614	$2\,^1S - 5\,^1P$, $5\,^1D$	3.15	9	0.83	0.52

In Table 1 are listed from the left to the right: wavelength λ, allowed (A) and forbidden (F) transition, separation Δ between A and F for vanishing electric field, ratio of Δ and $\omega = 2\pi \cdot 80\,\mathrm{GHz}$ (ω_{pe} for $n_e = 8 \cdot 10^{19}\,\mathrm{m}^{-3}$). Moreover, the intensity of F for $E_{rms} = 1\,\mathrm{kV/cm}$ and the intensity of the "near" satellite for $E_{rms} = 1\,\mathrm{kV/cm}$ and $\omega = 2\pi \cdot 80\,\mathrm{GHz}$ are given in per cent of the allowed line intensity.

III. Measurements and Interpretation of Line Profiles

a) The frequency spectrum of microfields

A microfield $E \cos \omega t$ gives rise to two satellites at $\pm\omega$ from the position of a forbidden line F. If the magnetic field is small, so that no splitting due to Zeeman effect occurs, the strength of the far (S_+) and near (S_-) satellite, relative to the intensity of a nearby allowed line A, is given for small electric fields by [2]

$$S_{\pm}^{BM}(\omega) = \text{const}\,\frac{\langle E^2(\omega)\rangle}{(\Delta \pm \omega)^2},$$

where Δ is the frequency separation of A and F. In Fig. 3 the measured profiles of two helium lines are presented. Two frequency domains of microfields can clearly be observed: low-frequency oscillations ($f < 10\,\mathrm{GHz}$) breaking the selection rules for dipole radiation, so that the forbidden line becomes visible. At the same time high-frequency oscillations with frequency close to the electron plasma frequency f_{pe} cause two satellites in the line profiles.

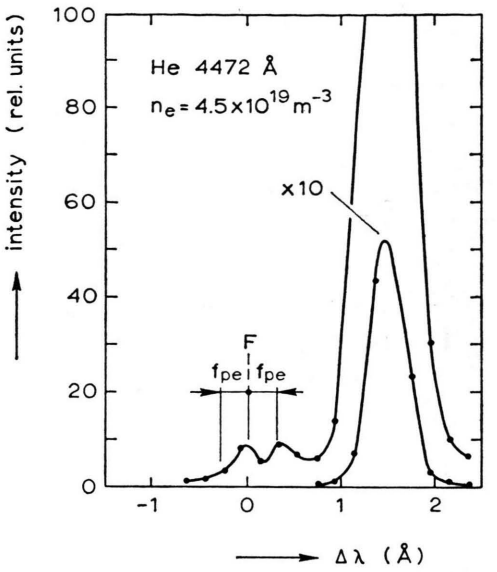

Fig. 3 b

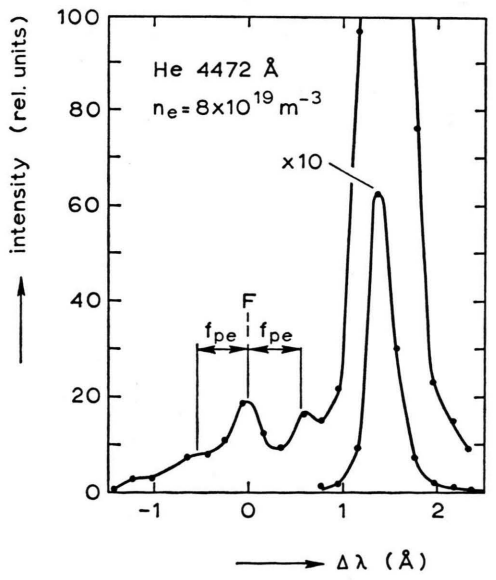

Fig. 3 a

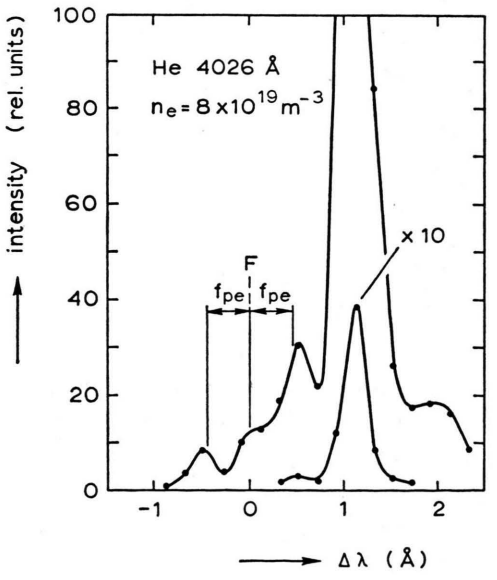

Fig. 3 c

Fig. 3. Measured helium line profiles without polarizer, and for a low-magnetic field, $t = 1 - 1.5\,\mu\mathrm{sec}$. The $2^3P - 4^3F$ forbidden line at 4470 Å is caused by low-frequency oscillations. High-frequency oscillations give rise to satellites at $\pm f_{pe}$ shown in a) for $n = 8 \cdot 10^{19}\,\mathrm{m}^{-3}$ and b) for $n = 4.5 \cdot 10^{19}\,\mathrm{m}^{-3}$. In c) this is shown for the $2^3P - 5^3F$ forbidden line. Note that in a) and b) the near satellite shifts with f_{pe}.

b) Orientation of microfields

The dominant polarization of the electric field can be concluded from the Zeeman pattern of the forbidden line and the satellites [4, 5]. Figures 4, 5, and 6 show the Zeeman pattern of the transition $2\,^1P - 4\,^1D$, F in neutral helium for three increasing values of the confining magnetic mirror field. The measurements are compared with Zeeman patterns as given by Hicks, Hess, and Cooper [5]. Good agreement between theory and experiment was found for random direction of h.f.-fields (five σ-components and three π-components) and l.f.-fields with dominant polarization perpendicular to the magnetic field direction (three σ-components and two π-components).

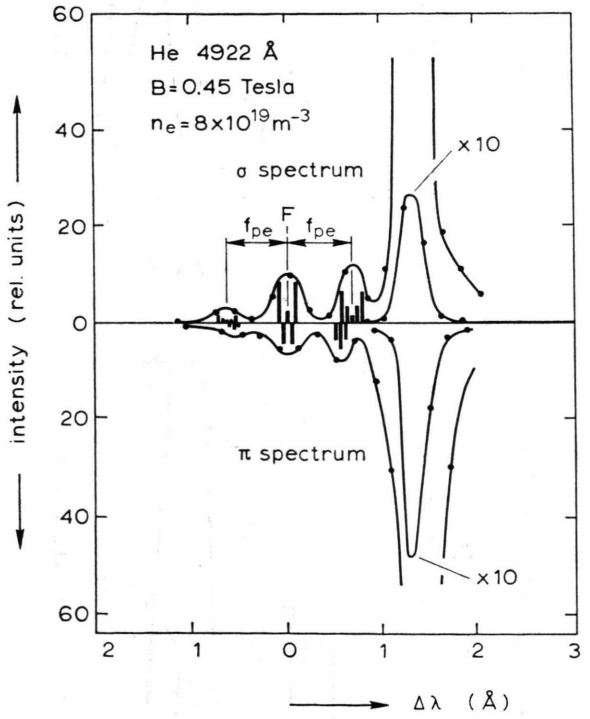

Fig. 4. The Zeeman pattern of 2^1P-4^1F and its satellites measured in parallel (π) and perpendicular (σ) polarization. The theoretical Zeeman pattern, denoted by vertical bars, is taken from Ref. 5 for random high-frequency fields (5 σ-components and 3 π-components). The low-frequency field is perpendicular to the B field and random in azimuth (3 σ-components and 2 π-components).

c) The field strength of high-frequency fields

The integrated intensity of satellites, separated by a frequency close to the electron plasma frequency f_{pe} from the forbidden line, is a direct measure for

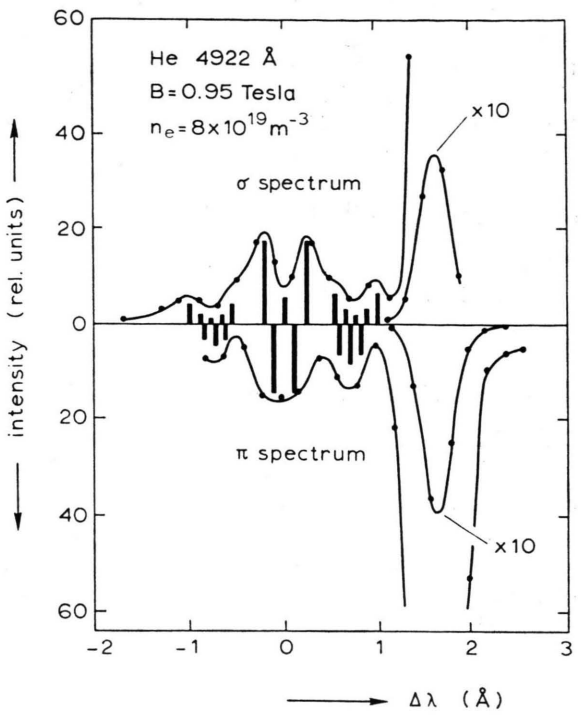

Fig. 5. As Fig. 4 for $B=0.95$ Tesla; $n_e=8\cdot10^{19}\,m^{-3}$, $E_0=47.5\,kV\,m^{-1}$.

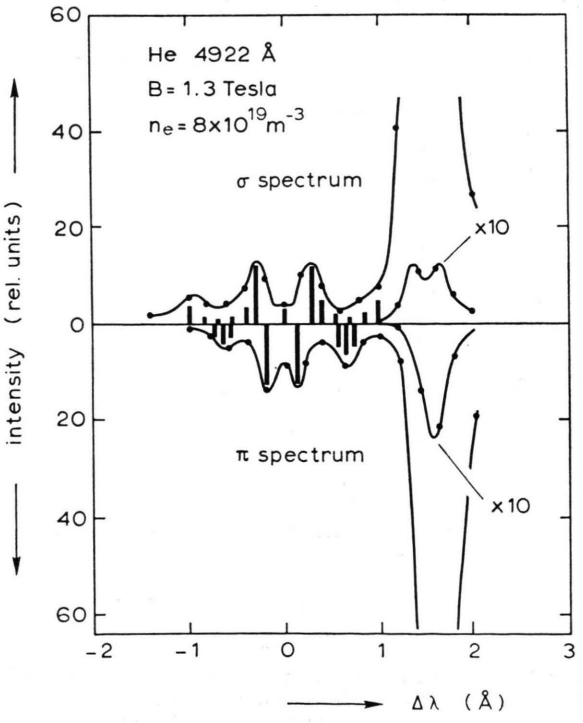

Fig. 6. As Fig. 4 for $B=1.3$ Tesla.

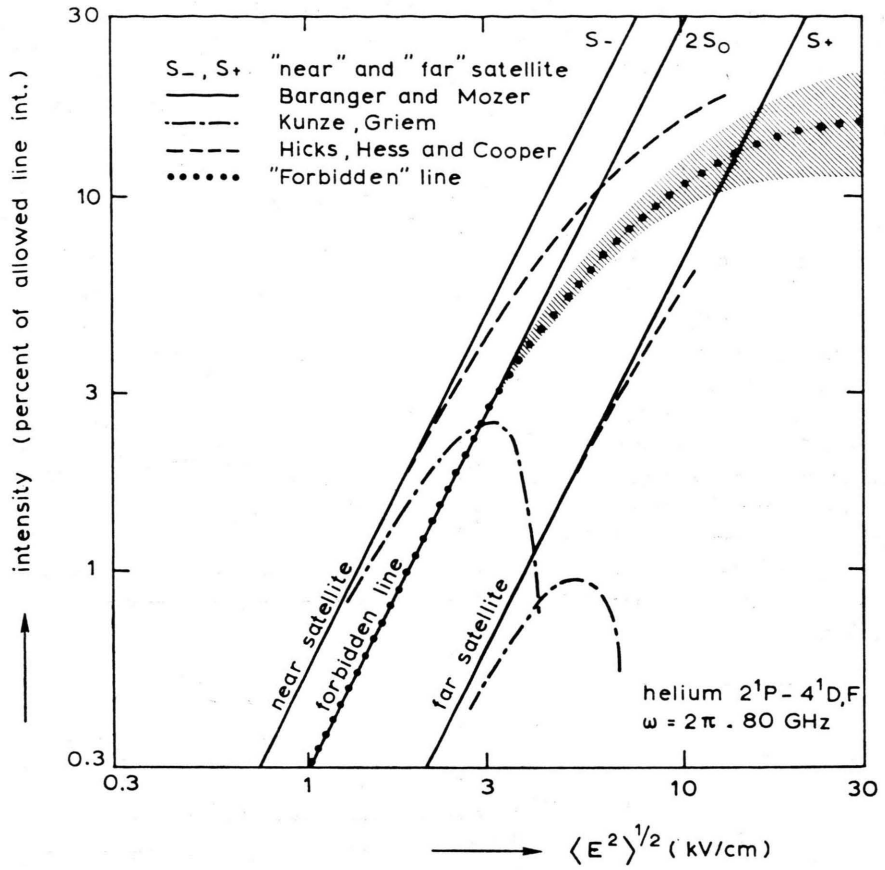

Fig. 7. Intensity of forbidden line and satellites versus the mean value of the low- and high-frequency electric field, respectively.
——— line: Second-order time-dependent perturbation theory (Ref. 2).
— · — · line: Higher-order perturbation theory (Ref. 1).
— — — line: Multilevel theory (Ref. 5).
····· line: Intensity of the forbidden line. The shaded area indicates the uncertainty in the relative intensity.

the strength of the electron Langmuir oscillations. For fields below a few kV/cm the formula of Baranger and Mozer can be used to deduce the field strength from the strength of the far (S_+^{BM}) and near (S_-^{BM}) satellite. For higher field strength the perturbation theory was extended to higher order by Kunze et al.[7] (a corrected expression for $S_\pm$ can be found in Ref. 1). Different data (only for $2\,^1P - 4\,^1D, F$) from multilevel theory were published by Hicks, Hess, and Cooper[5]. In Fig. 7 the results from second-order perturbation theory, higher-order perturbation theory, and multilevel theory are compared for $\lambda = 4922$ Å and $\omega = 2\pi \cdot 80$ GHz ($2.7\ \mathrm{cm}^{-1}$). The higher-order perturbation theory predicts a vanishing intensity of the near satellite for fields in excess of 4 kV/cm, while the maximum intensity is below 3%. This behaviour was not found in the experiment. We therefore used the results from multilevel theory taken from Ref. 5 to calculate the strength of electric fields from the intensity of satellites, denoted as a broken line in Figure 7. In Fig. 9 the high-frequency field strength, E_{hf}, calculated from R_- (Fig. 9b) and R_+ (Fig. 9c) is given as a function of time for a typical experiment.

d) Strength of low-frequency fields

The strength of the low-frequency field can be determined from the formula of Baranger and Mozer in the limit of $\omega \to 0$ (multiplied by 2 because near and far satellite merge into one forbidden line) on the condition that the intensity is not larger than a few per cent of the allowed line. If the field is stronger the Stark shifts of allowed and forbidden line can be used for the determination of a mean value of the electric field. The experimental values for $\lambda = 4471$ Å found by Drawin and Ramette[14] and for 4922 Å found in Ref. 8 were considerably less (factor $2-3$) than theoretical values of the quadratic Stark shifts for fields of the order of 5 kV/cm, so caution is needed. For electric fields in excess of 30 kV/cm the shift becomes linear in the field. The

field strength of low-frequency oscillations was measured accurately in hydrogen plasmas (see Ref. 13). Values between 20 kV/cm and 50 kV/cm were found. We used this knowledge in an experiment in which helium was added as a tracer in a hydrogen discharge. The r.m.s. electric field is 25 kV/cm in a pure hydrogen discharge for plasma parameters of Figure 8. A value of 20 kV/cm is deducted from the Stark shifts of allowed and forbidden line for the mixture. The measured intensity of $12^1/_2\%$ for the forbidden line is a lower limit for $2\,S_0$ at this field strength because the allowed line can be intensified by light from the cold plasma boundary. This intensity is far below the value calculated from the Baranger-Mozer formula. Note in Fig. 8 the higher-order satellites at f_{pe} and $2\,f_{pe}$ from the allowed line indicating the presence of a strong high-frequency field at the same time. The relation between the field strength of the low-frequency field and the intensity of the forbidden line $2\,^1P - 4\,^1F$ used in this paper is shown in Fig. 7 as a dotted line.

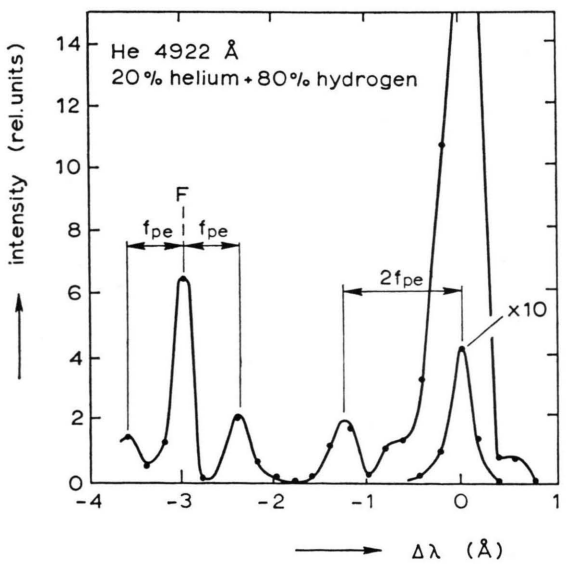

Fig. 8. Profile of the $2^1P-4^1D, F$ transition. $E_{rms}=25$ kV cm^{-1} in a pure hydrogen discharge. In the hydrogen helium mixture the field strength calculated from the Stark shifts of allowed and forbidden line is 20 kV cm^{-1}. Note the satellites at $\pm f_{pe}$ from the forbidden line and $2\,f_{pe}$ (and even f_{pe}) from the allowed line.

In Fig. 9 E_{lf} (9 a) and E_{hf} (9 b and 9 c) are given as a function of time for three different values of the magnetic field. Field strengths between 2 kV/cm and 10 kV/cm were found. The time dependence of the low-frequency field is weak where the high-frequency field increases with time and reaches at the end of the turbulent heating phase ($t\sim 3\,\mu$sec) the value of the low-frequency field. The energy level of the fluctuations is a factor of 3 lower than in hydrogen experiments (Ref. 13). This is plausible because the effective collision frequency is lower for helium and the arc cross section, energy losses and drift velocity are slightly different.

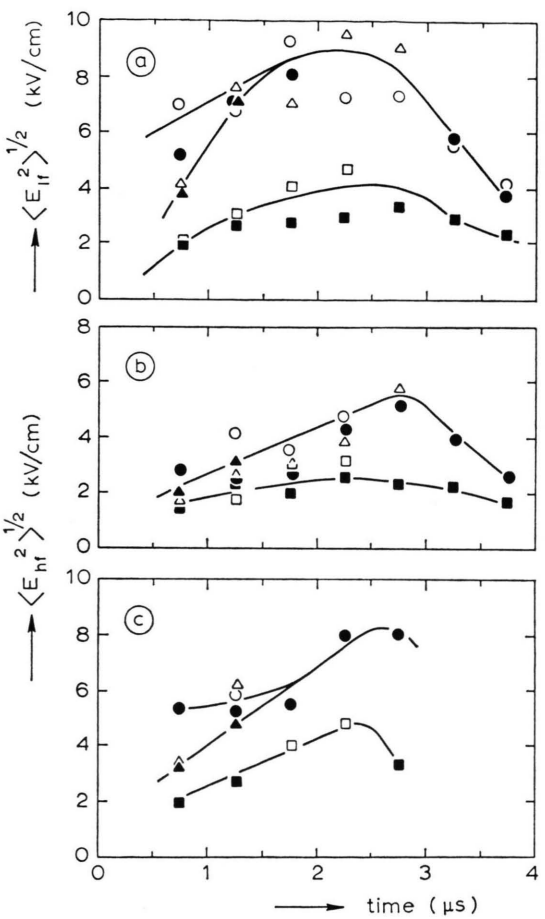

Fig. 9. a) Calculated field strength of low-frequency fields from the intensity of the forbidden line 2^1P-4^1F as a function of time. b) Calculated high-frequency ($f\sim f_{pe}$) field strength from the intensity of the near satellite. c) Idem from the far satellite. Square: magnetic field 0.45 Tesla; ■ parallel polarization; □ perpendicular polarization. Triangle: magnetic field 0.95 Tesla; Circle: magnetic field 1.3 Tesla.

IV. Discussion

The inspection of the Stark-Zeeman pattern of forbidden lines and its satellites is a useful diagnostic method for the determination of the frequency spec-

trum and direction of microfields, as was shown in Sect. III a and III b. On the other hand the strength of the fields must be calculated with caution. Firstly, the intensity of the allowed line can be overestimated due to light from the plasma boundary. Because of the observed quadratic Stark shift of about 0.3 Å for $\lambda = 4472$ Å and $\lambda = 4922$ Å the line is certainly not overshadowed by light from outside the turbulent region. Secondly, the occupation of upper levels may depart from thermal equilibrium. The relative population of the 4 F and 4 D levels is not known in our experiment. Burrell and Kunze[15] measured strong collisional coupling between all $n = 4$ levels and found that the density of atoms in a state is according to its statistical weight. For our plasma we have insufficient data for direct electron excitation of the upper state and for excitation and collisional transfer between them to calculate the (relative) population of levels. This may lead to an underestimation of the calculated field strengths by a factor of 2.

Thirdly, the selection rules for two (multi) photon transitions are violated if the electron orbits are deformed by a (quasi-) static electric field. This was noted already in the description of Fig. 8 and is clearly demonstrated in Fig. 10 where a strong high-

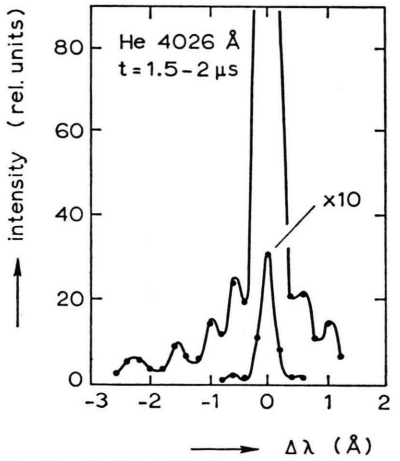

Fig. 10. Profile of $2^3P-5^3D, F$ perturbed by strong Langmuir turbulence. The frequency difference between the intensity maxima is close to f_{pe}.

frequency field causes a series of satellites at $n \cdot f_{pe}$ from the allowed (and forbidden?) line. The high-frequency field strength was measured from the profile of the hydrogen like He II 4686 Å line (see Figure 11). From the decrease of the satellites at $n \cdot f_{pe}$ a field strength of 12 kV/cm is calculated. The

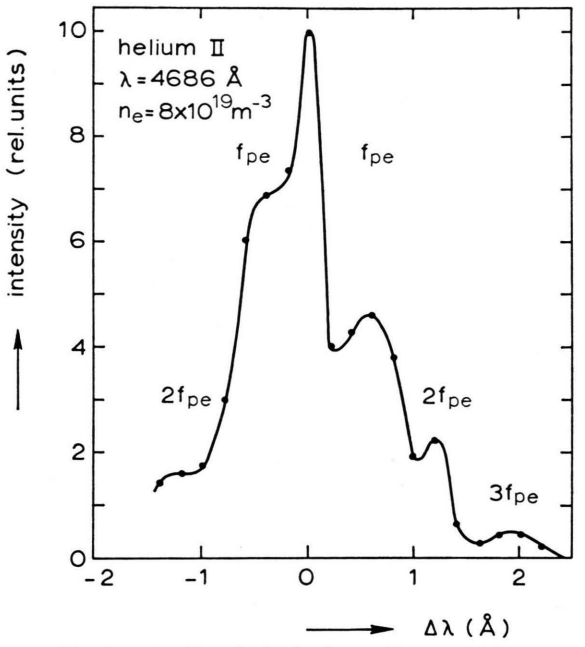

Fig. 11. Profile of the hydrogen-like transition $n = 4 \rightarrow n' = 3$ in single ionized helium.

perturbation of a helium neutral by this high-frequency field and a low-frequency field of comparable strength leads to the complicated spectral profile of Fig. 10 which cannot be interpreted with existing theories. In conclusion we have shown that the spectral profile of forbidden helium lines contains valuable information on turbulent microfields. The energy density in the waves amounts to 1‰ of the thermal energy density in a heating experiment. The level of the wave energy is consistent with the measured anomalous resistivity (Ref. 12) where the frequency spectrum shows the existence of both ion-acoustic waves and Langmuir oscillations.

Acknowledgement

The author is grateful to Dr. H. de Kluiver for his encouragement and support during this work. The author also wishes to thank Prof. C. M. Braams and Drs. H. W. Kalfsbeek for valuable discussions. The author is indebted to Mr. R. A. A. Ambags for assistance in the optical measurements and to Mr. H. W. van der Ven for the measurement of the Bremsstrahlung.

This work was performed as part of the research programme of the association agreement of Euratom and the "Stichting voor Fundamenteel Onderzoek der Materie" (FOM) with financial support from the "Nederlandse Organisatie voor Zuiver-Wetenschappelijk Onderzoek" (ZWO) and Euratom.

[1] H. R. Griem, Spectral Line Broadening by Plasmas, John Wiley, New York 1974.
[2] M. Baranger and B. Mozer, Phys. Rev. **123**, 25 [1961].
[3] W. S. Cooper and H. Ringler, Phys. Rev. **179**, 226 [1969].
[4] W. S. Cooper and R. A. Hess, Phys. Rev. Lett. **25**, 433 [1970].
[5] W. W. Hicks, R. A. Hess, and W. S. Cooper, Phys. Rev. **A 5**, 490 [1972].
[6] L. Klein, M. Giraud, and A. Ben-Reuven, Phys. Rev. **A 10**, 682 [1974].
[7] H. J. Kunze, H. R. Griem, A. W. de Silva, G. C. Goldenbaum, and I. J. Spalding, Phys. Fluids **12**, 2669 [1969]; W. D. Davis, Phys. Fluids **15**, 2383 [1972].
[8] F. R. Scott, R. V. Neidigh, J. R. McNally, and W. S. Cooper, J. Appl. Phys. **41**, 5327 [1970].
[9] D. R. Matt and F. R. Scott, Phys. Fluids **15**, 1047 [1972].
[10] H. Schrijver et al., Proc. 5th Inf. Conf. on Plasma Phys. and Contr. Nuclear Fusion Res., Tokyo, November 1974, CN 33/C3-1.
[11] H. W. Piekaar, Plasma Physics **15**, 565 [1973].
[12] H. Schrijver, Physica **70**, 358 [1973].
[13] W. R. Rutgers and H. de Kluiver, Z. Naturforsch. **29 a**, 42 [1974]. — W. R. Rutgers and H. W. Kalfsbeek, Z. Naturforsch. **30 a**, 739 [1975].
[14] H. W. Drawin and J. Ramette, Z. Naturforsch. **29 a**, 838 [1974].
[15] C. F. Burrell and H. J. Kunze, Phys. Rev. Lett. **28**, 1 [1972].